Eur Phys J A (2005) **24,** s2, 47–50
DOI: 10.1140/epjad/s2005-04-010-6

EPJ A direct
electronic only

Parity violating electron scattering at the MAMI facility in Mainz

The strangeness contribution to the form factors of the nucleon

F.E. Maas, for the A4-Collaboration

Johannes Gutenberg Universität Mainz,
Institut für Kernphysik, J.J.Becherweg 45, 55299 Mainz, Germany
e-mail: maas@kph.uni-mainz.de

Received: 15 December 2004 / Published Online: 8 February 2005

Abstract. We report here on a new measurement of the parity violating (PV) asymmetry in the scattering of polarized electrons on unpolarized protons performed with the setup of the A4-collaboration at the MAMI accelerator facility in Mainz. This experiment is the first to use counting techniques in a parity violation experiment. The kinematics of the experiment is complementary to the earlier measurements of the SAMPLE collaboration at the MIT Bates accelerator and the HAPPEX collaboration at Jefferson Lab. After discussing the experimental context of the experiments, the setup at MAMI and preliminary results are presented.

PACS. 12.15 Electroweak interactions – 11.30.Er Charge conjugation, parity, time reversal, and other discrete – 13.40.Gp Electromagnetic form factors – 25.30.Bf Elastic electron scattering

1 Strangeness in the nucleon

The understanding of quantum chromodynamics (QCD) in the nonperturbative regime of low energy scales is crucial for understanding the structure of hadronic matter like protons and neutrons (nucleons). The successful description of a wide variety of observables by the concept of effective, heavy (≈ 350 MeV) constituent quarks, which are not the current quarks of QCD, is still a puzzle. There are other equivalent descriptions of hadronic matter at low energy scales in terms of effective fields like chiral perturbation theory (χPT) or Skyrme-type soliton models. The effective fields in these models arise dynamically from a sea of virtual gluons and quark-antiquark pairs. In this context the contribution of strange quarks plays a special role since the nucleon has no net strangeness, and any contribution of strange quarks to the nucleon structure observables is a pure sea-quark effect. Due to the heavier current quark mass of strangeness (m_s) as compared to up (m_u) and down (m_d) with $m_s \approx 140$ MeV $\gg m_u, m_d \approx$ 5-10 MeV, one expects a suppression of strangeness effects in the creation of quark-antiquark pairs. On the other hand the strange quark mass is in the range of the mass scale of QCD ($m_s \approx \Lambda_{QCD}$) so that the dynamic creation of strange sea quark pairs could still be substantial. The topic of the strangeness content of the nucleon has been widely discussed in other contributions to this conference from J. Ellis, A. Silva, B. Kubis and others. Parity violating (PV) electron scattering off nucleons provides experimental access to the strange quark vector current in the nucleon $\langle N|\bar{s}\gamma_\mu s|N\rangle$ which is parameterized in the electromagnetic form factors of proton and neutron, G_E^s and G_M^s [1]. Recently the SAMPLE-, HAPPEX- and A4-collaboration have published experimental results. A direct separation of electric (G_E^s) and magnetic (G_M^s) contribution at forward angle has been impossible so far, since the measurements have been taken at different Q^2-values. The experimental details of the SAMPLE, HAPPEX, A4 and G0 collaboration is discussed in greater detail in many long and short contributions of this conference proceedings.

A determination of the weak vector form factors of the proton ($\tilde{G}_E^p$ and $\tilde{G}_M^p$) by measuring the PV asymmetry in the scattering of longitudinally polarized electron off unpolarized protons allows the determination of the strangeness contribution to the electromagnetic form factors G_E^s and G_M^s. The weak vector form factors $\tilde{G}_{E,M}^p$ of the proton can be expressed in terms of the known electromagnetic nucleon form factors $G_{E,M}^{p,n}$ and the unknown strange form factors $G_{E,M}^s$ using isospin symmetry and the universality of the quarks in weak and electromagnetic interaction $\tilde{G}_{E,M}^p = (G_{E,M}^p - G_{E,M}^n) - 4\sin^2\theta_W\, G_{E,M}^p - G_{E,M}^s$. The interference between weak (Z) and electromagnetic (γ) amplitudes leads to a PV asymmetry $A_{LR}(\mathbf{e}p) = (\sigma_R - \sigma_L)/(\sigma_R + \sigma_L)$ in the elastic scattering cross section of right- and left-handed electrons (σ_R and σ_L respectively), which is given in the framework of the Standard Model [2]. $A_{LR}(\mathbf{e}p)$ is of order parts per million (ppm). The asymmetry can be expressed as a sum of three terms, $A_{LR}(\mathbf{e}p) = A_V + A_s + A_A$. A_V represents the vector coupling at the proton vertex where the possible strangeness contribution

has been taken out and has been put into A_s, a term arising only from a contribution of strangeness to the electromagnetic vector form factors. The term A_A represents the contribution from the axial coupling at the proton vertex due to the neutral current weak axial form factor $\tilde{G}_A^p$. We average $A_0 = A_V + A_A$ over the acceptance of the detector and the target length in order to calculate the expected asymmetry. The largest contribution to the uncertainty of A_0 comes from the uncertainty in the axial form factor G_A, the electric form factor of the proton G_E^p, and the magnetic form factor of the neutron G_M^n.

2 The A4 experimental setup and analysis

The A4 experiment at MAMI is complementary to other experiments since for the first time counting techniques have been used in a scattering experiment measuring a PV asymmetry. Therefore possible systematic contributions to the experimental asymmetries and the associated uncertainties are of a different nature as compared to previous experiments, which use analogue integrating techniques. More details on the A4 apparatus can be found in the contributions of J. Diefenbach, B. Gläser, Y. Imai, J. H. Lee and C. Weinrich.

The PV asymmetry was measured at the MAMI accelerator facility in Mainz [3] using the setup of the A4 experiment [4]. The polarized 570.4 and 854.3 MeV electrons were produced using a strained layer GaAs crystal that is illuminated with circularly polarized laser light [5]. Average beam polarization was about 80 %. The helicity of the electron beam was selected every 20.08 ms by setting the high voltage of a fast Pockels cell according to a randomly selected pattern of four helicity states, either $(+P-P-P+P)$ or $(-P+P+P-P)$. A 20 ms time window enabled the histogramming in all detector channels and an integration circuit in the beam monitoring and luminosity monitoring systems. The exact window length was locked to the power frequency of 50 Hz in the laboratory by a phase locked loop. For normalization, the gate length was measured for each helicity. Between each 20 ms measurement gate, there was an 80 μs time window for the high voltage at the Pockels cell to be changed. The intensity $I = 20$ μA of the electron current was stabilized to better than $\delta I/I \approx 10^{-3}$. An additional $\lambda/2$-plate in the optical system was used to rotate small remaining linear polarization components and to control the helicity correlated asymmetry in the electron beam current to the level of < 10 ppm in each five minute run.

From the source to the target, the electron beam develops fluctuations in beam parameters such as position, energy and intensity which are partly correlated to the reversal of the helicity from +P to -P. We have used a system of microwave resonators in order to monitor beam current, energy, and position in two sets of monitors separated by a drift space of about 7.21 m in front of the hydrogen target. In addition, we have used a system of 10 feed-back loops in order to stabilize current, energy [6], position, and angle of the beam. The polarization of the electron beam was measured with an accuracy of 2 % using a Møller polarimeter

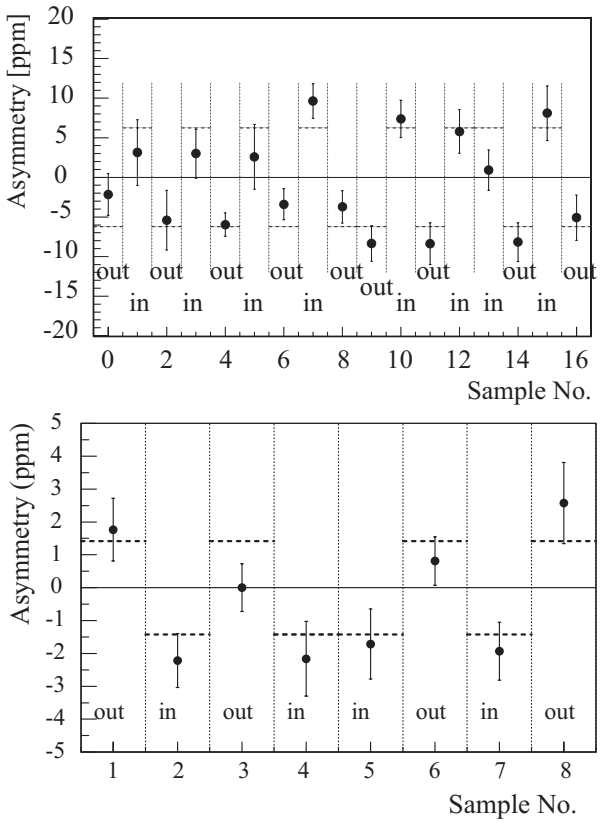

Fig. 1. The *top plot* shows the data samples of 854.3 MeV data with the $\lambda/2$-plate in and out. The *lower plots* represents the data sample for the 570.4 MeV data with the $\lambda/2$-plate in and out as described in the text

which is located on a beam line in another experimental hall [7]. Due to the fact that we had to interpolate between the weekly Møller measurements, the uncertainty in the knowledge of the beam polarization increased to 4 %. The 10 cm high power, high flow liquid hydrogen target was optimized to guarantee a high degree of turbulence with a Reynolds-number of $R > 2 \times 10^5$ in the target cell in order to increase the effective heat transfer. For the first time, a fast modulation of the beam position of the intense CW 20 μA beam could be avoided. It allowed us to stabilize the beam position on the target cell without target density fluctuations arising from boiling. The total thickness of the entrance and exit aluminum windows was 250 μm. The luminosity L was monitored for each helicity state (R, L) during the experiment using eight water-Cherenkov detectors (LuMo) that detect scattered particles symmetrically around the electron beam for small scattering angles in the range of $\theta_e = 4.4^\circ - 10^\circ$, where the PV asymmetry is negligible. The photomultiplier tube currents of these luminosity detectors were integrated during the 20 ms measurement period by gated integrators and then digitized by customized 16-bit analogue-to-digital converters (ADC). The same method was used for all the beam parameter signals. A correction was applied for the nonlinearity of the luminosity monitor photomultiplier tubes. From the beam current helicity pair data $I^{R,L}$ and lumi-

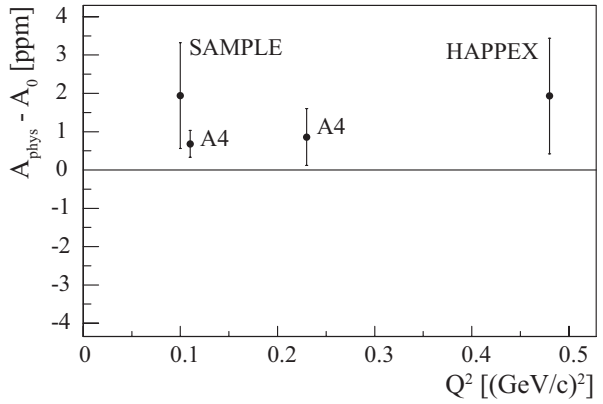

Fig. 2. Difference between the measured parity violating asymmetry in electron proton scattering $A_{LR}(\mathbf{e}p)$ and the asymmetry A_0 without vector strangeness contribution from the Standard Model for the SAMPLE experiment at *backward angles*, and the HAPPEX and the two A4 results at *forward angles*. The new experimental result at Q^2=0.108 (GeV/c)^2 presented here is the most accurate measurement

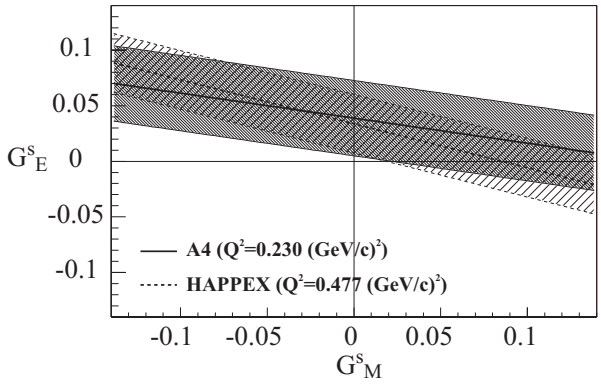

Fig. 3. The *solid line* represents all possible combinations of $G_E^s + 0.225 G_M^s$ as extracted from the work presented here at a Q^2 of 0.230 (GeV/c)^2. The densely hatched region represents the 1-σ uncertainty. The recalculated result from the HAPPEX published asymmetry at Q^2 of 0.477 (GeV/c)^2 is indicated by the *dashed line*, the less densely hatched area represents the associated error of the HAPPEX result

nosity monitor helicity pair $L^{R,L}$ data we calculated the target density $\rho^{R,L} = L^{R,L}/I^{R,L}$ for the two helicity states independently.

To detect the scattered electrons we developed a new type of a very fast, homogeneous, total absorption calorimeter consisting of individual lead fluoride (PbF_2) crystals [8,9]. The material is a pure Cherenkov radiator and has been chosen for its fast timing characteristics and its radiation hardness. This is the first time this material has been used in a large scale calorimeter for a physics experiment. The crystals are dimensioned so that an electron deposits 96 % of its total energy in an electromagnetic shower extending over a matrix of 3×3 crystals. Together with the readout electronics this allows us a measurement of the particle energy with a resolution of $3.9\,\%/\sqrt{E}$ and a total dead time of 20 ns. For the data taken at 854.3 MeV only 511 out of 1022 channels of the detector and the readout electronics were operational, for the 570.4 MeV data all the 1022 channels were installed. The particle rate within the acceptance of this solid angle was $\approx 50 \times 10^6$ s^{-1}. Due to the short dead time, the losses due to double hits in the calorimeter were 1 % at 20 μA. This low dead time is only possible because of the special readout electronics employed. The signals from each cluster of 9 crystals were summed and integrated for 20 ns in an analogue summing and triggering circuit and digitized by a transient 8-bit ADC. There was one summation, triggering, and digitization circuit per crystal. The energy, helicity, and impact information were stored together in a three dimensional histogram.

The number of elastic scattered electrons is determined for each detector channel by integrating the number of events in an interval from 1.6 σ_E above pion production threshold to 2.0 σ_E above the elastic peak in each helicity histogram, where σ_E is the energy resolution for nine crystals. These cuts ensure a clean separation between elastic scattering and pion production or Δ-excitation which has an unknown PV cross section asymmetry. The linearity of the PbF_2 detector system with respect to particle counting rates and possible effects due to dead time were investigated by varying the beam current. We calculate the raw normalized detector asymmetry as $A_{\rm raw} = (N_e^R/\rho^R - N_e^L/\rho^L)/(N_e^R/\rho^R + N_e^L/\rho^L)$. The possible dilution of the measured asymmetry by background originating from the production of π^0's that subsequently decays into two photons where one of the photons carries almost the full energy of an elastic scattered electron was estimated using Monte Carlo simulations to be much less than 1 % and is neglected here. The largest background comes from quasi-elastic scattering at the thin aluminum entrance and exit windows of the target cell. We have measured the aluminum quasi-elastic event rate and calculated in a static approximation a correction factor for the aluminum of 1.030 $\pm$ 0.003 giving a smaller value for the corrected asymmetry.

Corrections due to false asymmetries arising from helicity correlated changes of beam parameters were applied on a run by run basis. The analysis was based on the five minute runs for which the counted elastic events in the PbF_2 detector were combined with the correlated beam parameter and luminosity measurements. In the analysis we applied reasonable cuts in order to exclude runs where the accelerator or parts of the PbF_2 detector system were malfunctioning. The analysis is based on a total of 7.3×10^6 histograms corresponding to 4.8×10^{12} elastic scattering events for the 854.3 MeV data and $4.8 \cdot 10^6$ histograms corresponding to $2 \cdot 10^{13}$ elastic events for the 570.4 MeV data.

For the correction of helicity correlated beam parameter fluctuations we used multi-dimensional linear regression analysis using the data. The regression parameters have been calculated in addition from the geometry of the precisely surveyed detector geometry. The two different methods agree very well within statistics. The experimental asymmetry is normalized to the electron beam po-

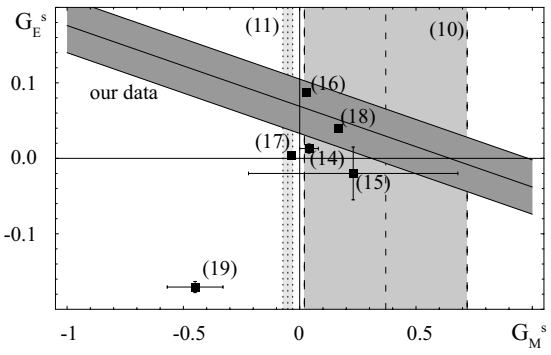

Fig. 4. The *solid lines* represent the result on $G_E^s + 0.106 G_M^s$ as extracted from our new data at $Q^2 = 0.108$ (GeV/c)^2 presented here. The hatched region represents in all cases the one-σ-uncertainty with statistical and systematic and theory error added in quadrature. The *dashed lines* represent the result on G_M^s from the SAMPLE experiment [10]. The *dotted lines* represent the result of a recent lattice gauge theory calculation for μ_s [11]. The boxes represent different model calculations and the numbers denote the references

larization P_e to extract the physics asymmetry, $A_{\rm phys} = A_{\rm exp}/P_e$. We have taken half of our data with a second $\lambda/2$-plate inserted between the laser system and the GaAs crystal. This reverses the polarization of the electron beam and allows a stringent test of the understanding of systematic effects. The effect of the plate can be seen in Fig. 1: the observed asymmetry extracted from the different data samples changes sign, which is a clear sign of parity violation if, as in our case, the target is unpolarized. Our measured result for the PV physics asymmetry in the scattering cross section of polarized electrons on unpolarized protons at an average Q^2 value of 0.230 (GeV/c)^2 is $A_{LR}(\mathbf{e}p) = (-5.44 \pm 0.54_{stat} \pm 0.26_{syst})$ ppm for the 854.3 MeV data [12] and $A_{LR}(\mathbf{e}p) = (-1.36 \pm 0.29_{stat} \pm 0.13_{syst})$ ppm for the 570.4 MeV data [13]. The first error represents the statistical accuracy, and the second represents the systematical uncertainties including beam polarization. The absolute accuracy of the experiment represents the most accurate measurement of a PV asymmetry in the elastic scattering of longitudinally polarized electrons on unpolarized protons. Figure 2 shows the present situation of all the published asymmetry measurements in elastic electron proton scattering. From the difference between the measured $A_{LR}(\mathbf{e}p)$ and the theoretical prediction in the framework of the Standard Model, A_0, we extract a linear combination of the strange electric and magnetic form factors for the 570.4 MeV data at a Q^2 of 0.108 (GeV/c)^2 of $G_E^s \pm 0.106\ G_M^s = 0.071 \pm 0.036$. For the data at 854.3 MeV corresponding to a Q^2 value of 0.230 (GeV/c)^2 we extract $G_E^s + 0.225\ G_M^s = 0.039 \pm 0.034$. Statistical and systematic error of the measured asymmetry and the error in the theoretical prediction of A_0 been added in quadrature. In Fig. 3 the results for the 570.4 MeV data are displayed. A recent very accurate determination of the strangeness contribution to the magnetic moment of the proton $\mu_s = G_M^s(Q^2 = 0\ (\mathrm{GeV/c})^2)$ from lattice gauge theory [11] would yield a larger value of $G_E^s = 0.076 \pm 0.036$ if the Q^2 dependence from 0 to 0.108 (GeV/c)^2 is neglected. The theoretical expectations for another quenched lattice gauge theory calculation [14], for SU(3) chiral perturbation theory [15], from a chiral soliton model [16], from a quark model [17], from a Skyrme-type soliton model [18] and from an updated vector meson dominance model fit to the form factors [19] are included into Fig. 4.

Our results concerning the measurement of the transverse beam spin asymmetry have been presented in the contribution of S. Baunack. We are also analyzing our data in the region of the $\Delta(1232)$ resonance, which has been presented in the contribution of L. Capozza. We are preparing a series of measurements of the parity violating asymmetry in the scattering of longitudinally polarized electrons off unpolarized protons and deuterons under backward scattering angles of $140^\circ < \theta_e < 150^\circ$ with the A4 apparatus in order to separate the electric (G_E^s) and magnetic (G_M^s) strangeness contribution to the electromagnetic form factors of the nucleon.

Acknowledgements. This work has been supported by the DFG in the framework of the SFB 201 and SPP 1034. We are indebted to K.H. Kaiser and the whole MAMI crew for their tireless effort to provide us with good electron beam. We are also indebted to the A1-Collaboration for the use of the Moeller polarimeter.

References

1. D.B. Kaplan et al.: Nucl. Phys. B **310**, 527 (1988)
2. M. Musolf et al.: Phys. Rep. **239**, 1 (1994)
3. H. Euteneuer et al.: Proc of the EPAC 1994 **1**, 506 (1994)
4. F.E. Maas et al.: Eur. Phys. J. A **17**, 339 (2003)
5. K. Aulenbacher et al.: Nucl. Ins. Meth. A **391**, 498 (1997)
6. M. Seidl et al.: Proc. of the EPAC 2000 , 1930 (2000)
7. P. Bartsch: Dissertation Mainz (2001)
8. F.E. Maas et al.: *Proc. of the ICATPP-7*, (World Scientific, 2002), p. 758
9. P. Achenbach et al.: Nucl. Ins. Meth. A **465**, 318 (2001)
10. D.T. Spayde et al.: Phys. Lett. B **583**, 79 (2004)
11. D.B. Leinweber et al.: hep-lat/0406002 (2004)
12. F.E. Maas et al.: Phys. Rev. Lett. **93**, 022002 (2004)
13. F.E. Maas et al.: nucl-ex/0412030 (2004)
14. R. Lewis et al.: Phys. Rev. D **67**, 013003 (2003)
15. T.R. Hemmert et al.: Phys. Rev. C **60**, 045501 (1999)
16. A. Silva et al.: Eur. Phys. J. A **22**, 481 (2004)
17. V. Lyubovitskij et al.: Phys. Rev. C **66**, 055204 (2002)
18. H. Weigel et al.: Phys. Lett. B **353**, 20 (1995)
19. H.-W. Hammer et al.: Phys. Rev. C **60**, 045204 (1999)